

# Multifurcated halogen bonding involving Ph–Cl⋯H–CPh=N–R' interactions and its relation to idioteloamphiphile layer architecture†‡

Rainer Glaser,\*<sup>a</sup> Richard F. Murphy,<sup>a</sup> Yongqiang Sui,<sup>a</sup> Charles L. Barnes<sup>ab</sup> and Sung Hoon Kim<sup>a</sup>

Received 31st January 2006, Accepted 12th April 2006

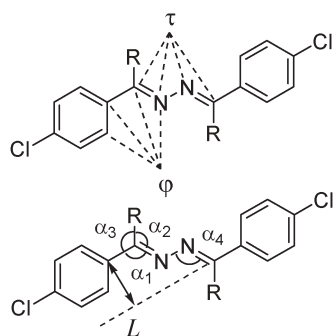
First published as an Advance Article on the web 26th April 2006

DOI: 10.1039/b601467d

The presence of halogen bonding between a chloroarene and an aldzine C–H bond, *i.e.* Ph–Cl⋯H–CPh=N–R', makes all the difference in the crystal structure of 4-chlorobenzaldazine (**1**, R = H) and causes an idioteloamphiphile layer architecture (flat with longitudinal offset) that features multifurcated halogen bonding and that differs drastically from the one in 4-chloroacetophenone azine (**2**, R = CH<sub>3</sub>).

Azines are 2,3-diazabutadienes and we have been interested in 1,4-diphenyl-2,3-diazabutadienes, X–Ph–CR=N–N=CR–Ph–Y. These materials form highly anisotropic layered structures and have proved invaluable for the construction of polar order in crystals of unsymmetrical azines ( $X \neq Y$ ).<sup>1–3</sup> Our studies focus on acetophenone azines (R = CH<sub>3</sub>) and we have studied both unsymmetrical<sup>4–7</sup> and symmetrical<sup>8–10</sup> azines. To understand the effects of the R-group on conformation and packing, we are investigating the benzaldehyde azines (R = H). Here we report an analysis of the crystal structure of 4-chlorobenzaldazine§,¶,|| (**1**, Scheme 1, Tables 1 and 2), provide results of *ab initio* theoretical studies<sup>11,12</sup> of isolated **1** (Table 1), and these data are discussed in comparison to the gas phase and crystal structures of 4-chloroacetophenone azine **2**.

Azines of the type X–Ph–CR=N–N=CR–Ph–Y almost always assume the (*E,E*)-configuration<sup>13</sup> and **1** and **2** are no exception.



**Scheme 1** Definition of torsion angles  $\tau$  and  $\phi$ , lateral offset (*LatOS*,  $l$ ), and bond angles,  $\alpha_i$ , for azines **1** (R = H) and **2** (R = Me).

<sup>a</sup>Department of Chemistry, University of Missouri-Columbia, Columbia, Missouri, 65211, USA. E-mail: glaser@missouri.edu

<sup>b</sup>Elmer O. Schlemper X-Ray Diffraction Center, University of Missouri-Columbia, Columbia, Missouri, 65211, USA

† Electronic supplementary information (ESI) available: CIF file, table with crystal data and information about the structure refinement, and results of electron density analyses of **1**. See DOI: 10.1039/b601467d

‡ This work was supported by the MU Research Board (RB #2358).

There is more variation in the conformations about the N–N and Ph–C bonds (Scheme 1).<sup>14,15</sup> Restricted Hartree–Fock calculations (RHF/6-31G\*) show that azine **1** is planar in the gas phase ( $\tau = 180^\circ$ ,  $\phi = 0^\circ$ ) and the X-ray structure analysis shows that **1** remains essentially planar in the crystal ( $\tau = 180^\circ$ ,  $\phi = 4.4^\circ$ , Table 1). The center of molecule **1** coincides with an inversion center ( $\tau = 180^\circ$ ) and this guarantees that the two phenyl rings are parallel. Moreover, the two phenyl rings in **1** are also essentially coplanar because the  $\phi$  angle is rather small. In contrast, **2** features significant N–N and Ph–C twists of  $\tau = 135^\circ$  and  $\phi = 31^\circ$ , respectively, and its two phenyl rings are nearly perpendicular to each other (Fig. 1). Table 1 shows agreement of the computed gas phase and the solid state structures of planar **1**. In the case of **2**, the  $C_{2h}$ -structure is a second-order saddle point,  $C_2$ -**2** is the minimum and slightly more stable than  $C_{2h}$ -**2** (by 0.25 kcal mol<sup>-1</sup>). Significant increases of  $\phi$  by *ca.* 12° and of  $\tau$  by *ca.* 19°, respectively, occur in the crystal and result in nearly perpendicular benzene planes. Fig. 1 illustrates the conformational differences. These comparisons are made at the RHF/6-31G\* level because this level was used in the earlier study of conformational properties of acetophenone azine conformation. With improved computational facilities available, we have now also determined the structure of **1** using second-order Møller–Plesset perturbation theory, in the frozen core approximation, and with the basis sets 6-31G\* and 6-311G\*\*. As can be seen from the data in Table 1, the structures are relatively independent of the theoretical level.

The R-group affects the  $\alpha_i$  angles about the azine backbone (Scheme 1, Table 1) and  $\alpha_1$  and  $\alpha_4$  control the lateral offset. The lateral offset (*LatOS*,  $l$ ) defines the distance between the arenes' local  $C_2$ -axes.<sup>16</sup> The lateral offset increases with a decrease of  $\alpha_1$  and an increase of  $\alpha_4$  and, therefore, the size of R affects both angles in a way to increase the lateral offset. The angle  $\alpha_1(\mathbf{1}) = 121^\circ$  is sort of normal while the methyl group reduces the angle to  $\alpha_1(\mathbf{2}) = 116^\circ$ . In contrast,  $\alpha_4(\mathbf{1}) = 112^\circ$  is less than  $\alpha_4(\mathbf{2}) = 115^\circ$ . The  $l$  values are 1.9 and 2.1 Å for crystals **1** and **2**, respectively, and both are less than in the gas phase.

Azines **1** and **2** both crystallize in space group  $P2_1/c$  and both form idioteloamphiphile layers (Fig. 2). However, the layer architectures and the mode of layer stacking differ greatly and far more than one might have anticipated based on the molecular properties of the azines. Note, in particular, that the small preference for the  $C_2$ -symmetric structure of **2** would not preclude a more or less planar structure in the crystal because the energy required for planarization is minute (Table 1). For the same reason, the preference for the  $C_{2h}$ -structure of **1** would not preclude a twisting of **1** in the solid state if such a twisting would provide for better intermolecular bonding.

**Table 1** Comparison of selected parameters for **1** and **2**

Parameter	X-Ray diffraction		RHF			MP2(fc)	
	<b>1</b>	<b>2</b>	6-31G* <b>1</b> , C <sub>2h</sub>	6-31G* <b>2</b> , C <sub>2h</sub>	6-31G* <b>2</b> , C <sub>2h</sub>	6-31G* <b>1</b> , C <sub>2h</sub>	6-311G** <b>1</b> , C <sub>2h</sub>
$\varphi$	4.4(2)	30.5	0	0	0	0	0
$\tau$	180	134.7	180	180	180	180	180
$\alpha_1$	121.02(12)	115.7	122.3	116.5	116.5	121.2	121.4
$\alpha_2$	119.5	124	120.3	125.4	125.4	120.1	120.0
$\alpha_3$	119.5	119.8	117.4	118	118	118.9	118.7
$\alpha_4$	111.86(14)	115.3	112.8	116.1	116.1	110.8	111.1
<i>LatOS</i> , <i>l</i>	1.96	2.06	1.90	2.26	2.26	1.97	1.96
Cl(1)–C(5)	1.7471(13)	1.74	1.74	1.74	1.74	1.74	1.74
C(1)–C(2)	1.4648(18)	1.48	1.47	1.5	1.5	1.46	1.46
C(1)–C(8)		1.49		1.51	1.51		
C(1)–N(1)	1.2772(18)	1.29	1.26	1.27	1.27	1.30	1.29
N(1)–N(1')	1.412(2)	1.4	1.38	1.38	1.38	1.41	1.40
<i>NIF</i>			0	2	2		
<i>E<sub>rel</sub></i> <sup>a</sup>				0.26	0.26		
<i>S</i>			126.63	128.6	128.6		
<i>TE</i>			148.20	186.5	186.5		
<i>G<sub>rel</sub></i> <sup>a</sup>				2.88	2.88		

<sup>a</sup> Relative energies  $E_{rel}$  and thermal energies  $TE$  in kcal mol<sup>-1</sup>, entropies  $S$  in cal mol<sup>-1</sup> K<sup>-1</sup>, and relative Gibbs free energy  $G_{rel}$  in kcal mol<sup>-1</sup>.

The layers of **2** feature complex longitudinal offsets in both layer directions (Fig. 2) and each azine **2** has two kinds of neighbors; those with a little and those with a substantial longitudinal offset (*LonOS*, *n*). The former engage in lateral double T-contacts<sup>17</sup> (*i.e.* twofold edge-to-face (effe) arene–arene interaction between two diarenes), lateral azine–azine contacts,<sup>18</sup> and lateral Cl⋯Cl halogen bonding. The offset azines interact *via* lateral Cl⋯(π)arene<sup>19</sup> and arene–azine interactions. The layers are stacked without alternation and interlayer interactions rely on Cl⋯Cl halogen bonding<sup>20</sup> and Cl⋯(π)arene interactions.

The planar azines **1** are stacked and the stacks are assembled into 2-D layers. Within the stacks, the azines engage in double face-to-face (ffff) arene–arene interactions with a stacking distance of  $d = 3.6$  Å, a parallel offset  $p = 1.5$  Å (Scheme 2), and lateral Cl⋯Cl halogen bonding. The long axes of the azines are slanted by about 45° relative to the layer surface (Fig. 2). In the direction of the slant, there is a very large longitudinal offset of  $n = 6.9$  Å and it is almost half of the azine's length of *ca.* 15 Å!

One consequence of the large offset is a lateral and intralayer interaction between the chlorine of one molecule and the azine's methylene and the benzene's *meta* hydrogen (relative to chlorine) of the next molecule. These two intralayer Cl⋯H–C(sp<sup>2</sup>) intermolecular bonds Cl⋯H<sub>a</sub>–C<sub>az</sub> and Cl⋯H<sub>b</sub>–Ph are highlighted in Fig. 3 and they occur between nearly coplanar neighbors. A second and equally important consequence of the large longitudinal offset relates to the fact that the layer surfaces no longer expose just chlorine atoms but the edges of phenyl rings now also appear on the layer surface. Fig. 1 illustrates very well that the H-atoms that are *ortho* with regard to chlorine (H<sub>c</sub>) appear on the layer surfaces. All surface chlorines engage in two interlayer interactions (Fig. 3). The Cl⋯H<sub>c</sub>–Ph and Cl⋯H<sub>c</sub>'–Ph interactions appear responsible for the alternation of the azines' tilt from layer to layer (Fig. 2). Thus, the overall result of the large longitudinal offset is a halogen bonding situation with multifurcation at the chlorine acceptor (Fig. 3). The two azines engaged in Cl⋯H<sub>a</sub>–C<sub>az</sub> and Cl⋯H<sub>b</sub>–Ph halogen bonding are almost coplanar. In contrast,

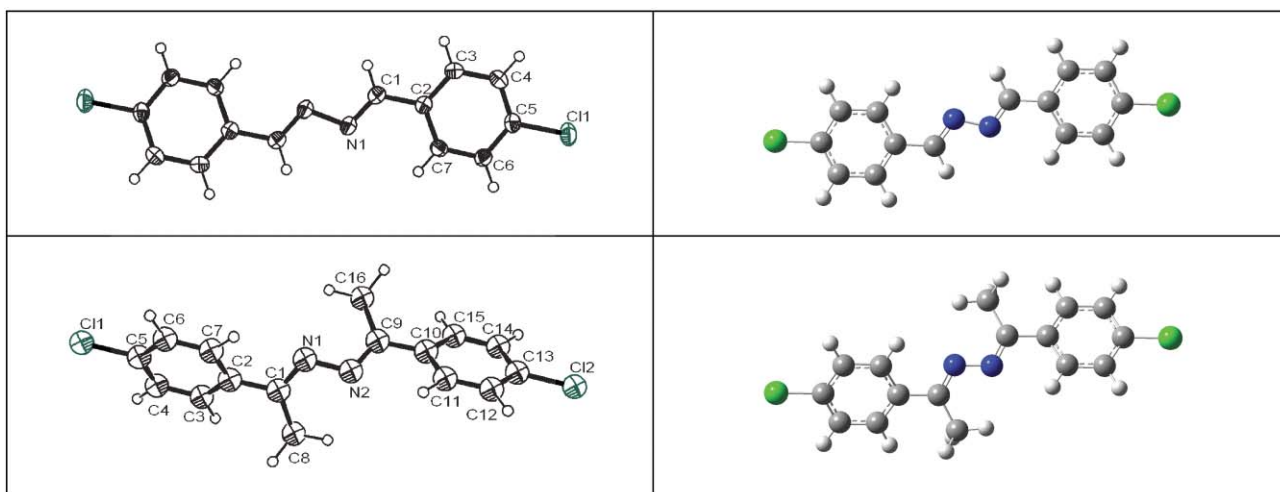


**Fig. 1** ORTEP3 drawings of **1** and **2** in the solid state with 50% thermal ellipsoid probability (left) and molecular models of their RHF/6-31G\* computed structures (right).

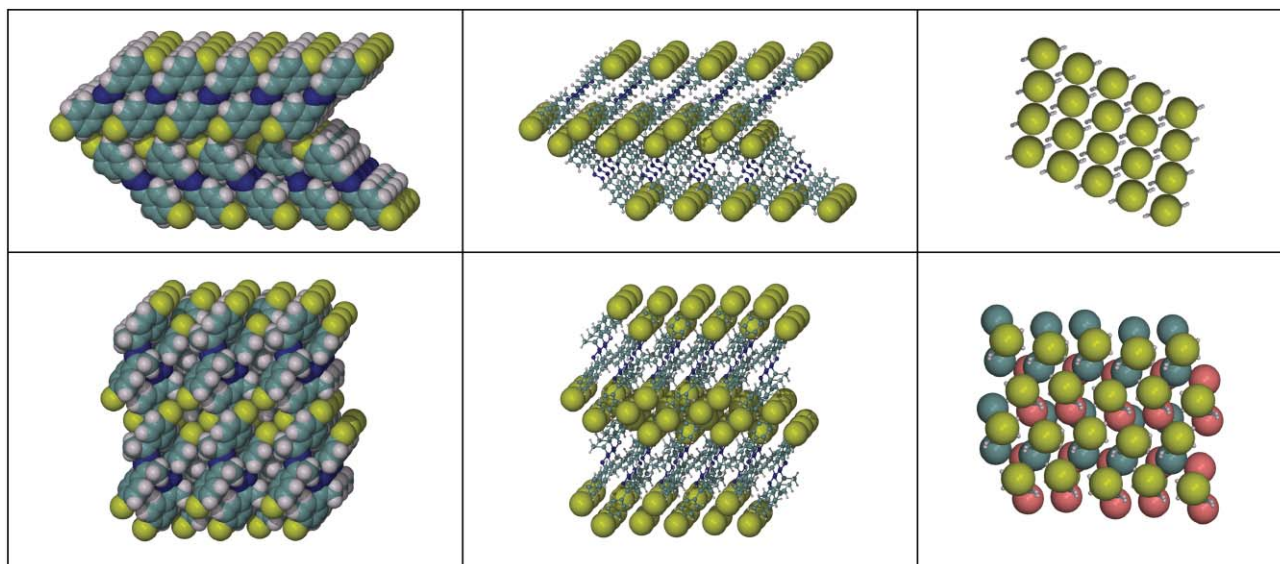
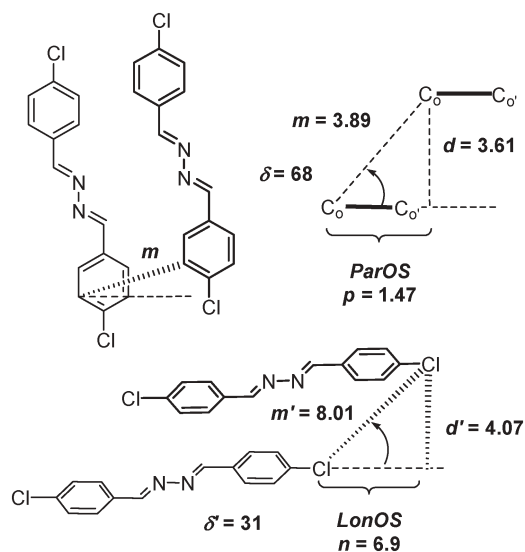


**Fig. 2** Layer architectures and layer stacking modes of **1** (top row) and **2**. In column 2, emphasis is placed on the chlorines (shown in yellow). In column 3, emphasis is placed on the chlorines (yellow) and the methyl groups of **2** (shown in green and red).

the  $\text{Cl}\cdots\text{H}_a'\text{-C}_{\text{az}}$  and  $\text{Cl}\cdots\text{H}_b'\text{-Ph}$  contacts involve molecules whose best planes are rather offset; these interactions are marginal, and neither the distance nor the angle criteria suggest significant  $\text{Cl}\cdots\text{H}_a'\text{-C}_{\text{az}}$  halogen bonding. Hence, it appears most reasonable to conclude that there are four good  $\text{C}\text{-Cl}\cdots\text{H}\text{-C}(\text{sp}^2)$  interactions in **1** with possibly a small contribution by a fifth contact. These  $\text{Cl}\cdots\text{H}\text{-C}(\text{sp}^2)$  interactions seem reasonable for purely structural reasons<sup>21</sup> because all of these  $\text{C}\text{-Cl}\cdots\text{H}\text{-C}$  contacts are shorter than 3.35 Å.<sup>22,23</sup> We determined the normalized hydrogen bonding distances  $R_{\text{HCl}} = d(\text{H}\cdots\text{Cl})/(r_{\text{H}} + r_{\text{Cl}})$  and found that the  $R_{\text{HCl}}^3$  values fall in the range 1.06–1.48 Å.<sup>24</sup> Since  $R_{\text{HCl}}^3 > 1$  and because all the  $R_{\text{HCl}}^3$  values are in the high-end of available statistical data, all  $\text{C}\text{-Cl}\cdots\text{H}\text{-C}(\text{sp}^2)$  contacts appear to be weak on structural grounds. Instead of optimizing one or two individual halogen bonds, the crystal architecture of **1**



**Scheme 2** Definitions of longitudinal offset (*LonOS*, *n*) and parallel offset (*ParOS*, *p*).

provides an excellent example of the benefits of multifurcated halogen bonding at the acceptor.

Some evidence is emerging in the literature for interactions that involve  $\text{C}(\text{sp}^2)\text{-H}$  bonds of aldehydes and of their derivatives.<sup>25,26</sup> Aldehyde H-atoms and the H-atoms of their N-analogs are rather deshielded<sup>27</sup> and the high chemical shifts might be caused by a significant electron density depletion and/or anisotropic effects of the environment (arene,  $\text{C}=\text{N}$ ). Hence, it is certainly not unreasonable to assume that the  $\text{Cl}\cdots\text{H}_a\text{-C}_{\text{az}}$  contact is attractive. To explore the nature of this interaction more deeply, we determined the electron density distribution of **1**, computed NBO charges<sup>28</sup> and analyzed molecular electrostatic potentials<sup>29</sup> at levels up to MP2/6-311G\*\*. The results are provided as supplementary material† and we briefly discuss the best data. All of the  $\text{C}(\text{sp}^2)$ -attached H-atoms are positively charged ( $\approx 0.2$ ) and the charge of  $\text{H}_a$  is *less* (0.16–0.17) than that of the arene H-atoms (0.20–0.21). The  $\text{C}_{\text{az}}$ -carbon is also positive ( $\approx 0.1$ ) while the arene C-atoms are negative (–0.10 – –0.22) and, thus, the  $\text{H}_a\text{C}_{\text{az}}$ -moiety is overall positive whereas all arene CH groups are close to neutral. The graphical illustration of the molecular electrostatic potential of **1** is shown in Fig. 4 and it reflects this charge distribution and informs the discussion with remarkable detail: The approach of a nucleophile to  $\text{H}_a$  is more likely from the “arene side” than the “azine side” and it is better to approach the H-atoms of the adjacent arene edge (including  $\text{H}_b$ ) than to approach  $\text{H}_a$ . Moreover, there is a pronounced preference for the approach of a donor to *one* arene edge, namely the edge that is on the side of the  $\text{H}_a\text{C}_{\text{az}}$ -moiety. Each and every  $\text{H}_c$  atom is on an arene edge shared with an  $\text{H}_b$ -atom. Hence, the new knowledge about the electrostatic properties of the azine supports and greatly strengthens the claim about  $\text{Cl}\cdots\text{H}_c\text{-Ph}$  and  $\text{Cl}\cdots\text{H}_c'\text{-Ph}$  interactions which was made above based on purely structural grounds. In fact, it was only after we learned that the arene edge presents an area of positive electrostatic potential that we fully recognized the significance to the  $\text{Cl}\cdots\text{H}_b\text{-Ph}$  interaction and, moreover, only then did we give any consideration to the fifth interaction, the  $\text{Cl}\cdots\text{H}_b'\text{-Ph}$  interaction.

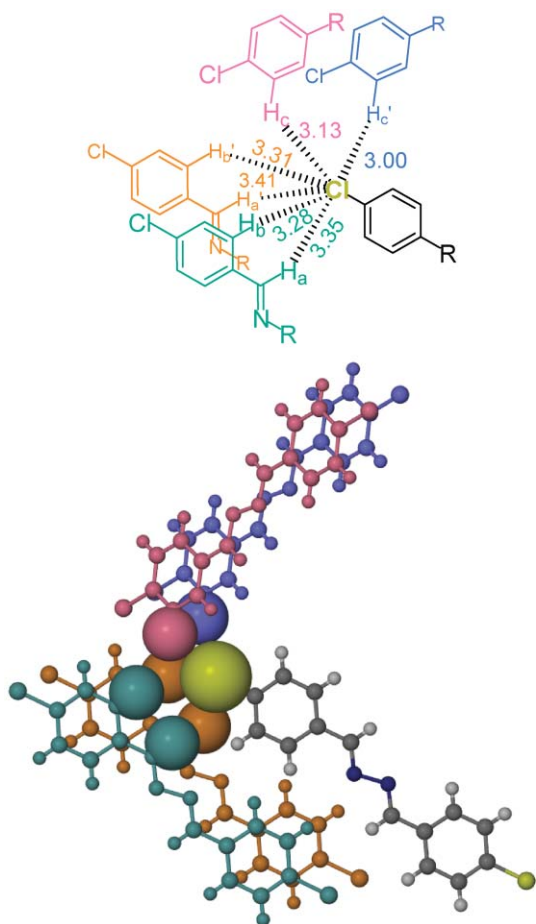


**Fig. 3** Chlorine contacts (in Å). Intralayer  $\text{Cl}\cdots\text{H}_a\text{-C}_{\text{az}}$ ,  $\text{Cl}\cdots\text{H}_a'\text{-C}_{\text{az}}$ ,  $\text{Cl}\cdots\text{H}_b\text{-Ph}$  and  $\text{Cl}\cdots\text{H}_b'\text{-Ph}$  contacts and interlayer  $\text{Cl}\cdots\text{H}_c\text{-Ph}$  and  $\text{Cl}\cdots\text{H}_c'\text{-Ph}$  interactions. Chlorine bonding angles are  $\angle(\text{C}_p\text{-Cl}\cdots\text{H}_a) = 98^\circ$ ,  $\angle(\text{C}_p\text{-Cl}\cdots\text{H}_a') = 79.7^\circ$ ,  $\angle(\text{C}_p\text{-Cl}\cdots\text{H}_b) = 141^\circ$ ,  $\angle(\text{C}_p\text{-Cl}\cdots\text{H}_b') = 118^\circ$ ,  $\angle(\text{C}_p\text{-Cl}\cdots\text{H}_c) = 143^\circ$  and  $\angle(\text{C}_p\text{-Cl}\cdots\text{H}_c') = 119^\circ$ . The H-atoms lie at the following equivalent positions:  $\text{H}_a$  is H1 and  $\text{H}_b$  is H3 of the azine at position  $(1 + x, 1 + y, z)$ ,  $\text{H}_a'$  is H1 and  $\text{H}_b'$  is H3 of the azine at  $(x, 1 + y, z)$ ,  $\text{H}_c$  is H4 of the azine at  $(2 - x, \frac{1}{2} + y, \frac{3}{2} - z)$ , and  $\text{H}_c'$  is H4 of the azine at  $(1 - x, \frac{1}{2} + y, \frac{3}{2} - z)$ .

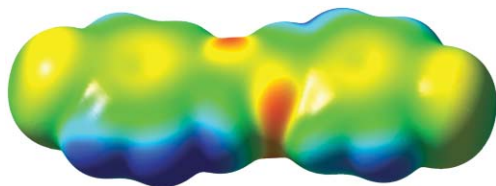


**Fig. 4** The electrostatic potential is mapped on the electron density isosurface of azine **1**. All properties were determined with the MP2/6-311G\*\* electron density; the isocontour surface is shown for  $0.0004 e$  (a.u.)<sup>-3</sup> and the electrostatic potential varies between  $-0.025$  (red) and  $+0.025$  (blue) a.u.

The structural analysis shows that **1** and **2** have similar lateral offsets and conformational analysis shows that **1** could easily adopt a conformation similar to **2** because the deformation energies are tiny. It is therefore reasonable to deduce that **1** could crystallize just like **2**. One must then deduce further that the actual structure of **1** is formed because it is thermodynamically favorable.

With everything else similar, the discussion suggests that the formation of  $\text{C}(\text{sp}^2)\text{-Cl}\cdots\text{H-C}(\text{sp}^2)$  contacts with a high degree of multifurcation at the acceptor (4–5) is a major determinant for the structure of **1**. In the case of **2**, one  $\text{Cl}\cdots\text{H-C}(\text{sp}^2)$  contact is absent ( $\text{Cl}\cdots\text{H}_a\text{-C}_{\text{az}}$ ) and another one would be sterically impeded ( $\text{Cl}\cdots\text{H}_b\text{-C}$ ) and, therefore, **2** realizes an alternative architecture with emphasis on more  $\text{Cl}\cdots\text{Cl}$  halogen bonding and  $\text{Cl}\cdots(\pi)$ arene interactions.

CCDC reference number 292918. For crystallographic data in CIF or other electronic format see DOI: 10.1039/b601467d

## Notes and references

§ 4-Chlorobenzaldazine was synthesized by condensation of hydrazine with two equivalents of 4-chlorobenzaldehyde in ethanol. The reaction was monitored until two equivalents of water had been formed in a Dean-Stark apparatus. The azine was purified by recrystallization and crystallized by slow diffusion from chloroform and cyclohexane. Crystal data were collected on a Bruker SMART CCD area detector. Cell refinement and data reduction were carried out with SAINT. Structure solution and refinement were performed with SHELXS/L.

¶ Chlorobenzaldazine crystal data:  $\text{C}_{14}\text{H}_{10}\text{Cl}_2\text{N}_2$ ,  $M = 277.14$ , monoclinic, cell dimensions (in Å)  $a = 3.8917(5)$ ,  $b = 6.9999(8)$ ,  $c = 22.977(3)$  Å,  $\beta = 90.798(2)^\circ$ ,  $V = 625.86(13)$  Å<sup>3</sup>,  $T = 173(2)$  K, space group =  $P2_1/c$ ,  $Z = 2$ , linear absorption coeff. = 0.499, reflections used: 3427,  $R_{\text{int}} = 0.0328$ ,  $R_{\text{final}} = 0.0348$  (all data).

|| We learned of the crystal structure report<sup>30</sup> of **1** at room temperature after the completion of this manuscript. Zheng, *et al.* describe some intramolecular features and our analysis of intermolecular bonding is complementary.

- 1 *Anisotropic Organic Materials - Approaches to Polar Order. ACS Symposium Series*, ed. R. Glaser and P. Kaszynski, vol. 798, American Chemical Society: Washington, D.C., 2001, pp. 97–111.
- 2 R. Glaser, N. Knotts and H. Wu, *ChemTracts*, 2003, **16**, 443–452.
- 3 R. Glaser, *Acc. Chem. Res.*, submitted.
- 4 G. S. Chen, J. K. Wilbur, C. L. Barnes and R. Glaser, *J. Chem. Soc., Perkin Trans. 2*, 1995, 2311–2317.
- 5 M. Lewis, C. L. Barnes and R. Glaser, *Acta Crystallogr., Sect. C*, 2000, **56**, 393–396.
- 6 M. Lewis, C. L. Barnes and R. Glaser, *J. Chem. Crystallogr.*, 2000, **30**, 489–496.
- 7 R. Glaser, N. Knotts, P. Yu, L. Li, M. Chandrasekhar, C. Martin and C. L. Barnes, *Dalton Trans.*, 2006, DOI: 10.1039/b515739k.
- 8 G. S. Chen, M. Anthamatten, C. L. Barnes and R. Glaser, *J. Org. Chem.*, 1994, **59**, 4336–4340.
- 9 M. Lewis, C. L. Barnes and R. Glaser, *J. Chem. Crystallogr.*, 1999, **29**, 1043–1048.
- 10 R. Glaser, G. S. Chen, M. Anthamatten and C. L. Barnes, *J. Chem. Soc., Perkin Trans. 2*, 1995, 1449–1458.
- 11 *Gaussian 03*, Revision D.01, M. J. Frisch *et al.*, Gaussian, Inc., Wallingford, CT, 2004.
- 12 C. J. Cramer, *Essentials of Computational Chemistry: Theories and Models*. John Wiley & Sons: New York, NY, 2002.
- 13 R. Glaser, G. S. Chen and C. L. Barnes, *J. Org. Chem.*, 1993, **58**, 7446–7455.
- 14 R. Glaser and G. S. Chen, *J. Comput. Chem.*, 1998, **19**, 1130–1140.
- 15 V. A. Sauro and M. S. Workentin, *J. Org. Chem.*, 2001, **66**, 831–838.
- 16 R. Glaser, L. R. Dendi, N. Knotts and C. L. Barnes, *Cryst. Growth Des.*, 2003, **3**, 291–300.
- 17 M. Lewis, Z. Wu and R. Glaser, *Arene–Arene Double T-Contacts. Lateral Synthons in the Engineering of Highly Anisotropic Organic Crystals*, ch. 7 in ref. 1.
- 18 R. Glaser, M. Lewis and Z. Wu, *J. Mol. Model.*, 2000, **6**, 86–98.
- 19 S. A. Cooke, C. M. Evans, J. H. Holloway and A. C. Legon, *J. Chem. Soc., Faraday Trans.*, 1998, **94**, 2295–2302.
- 20 P. Metrangolo, H. Neukirch, T. Pilati and G. Resnati, *Acc. Chem. Res.*, 2005, **38**, 386–395.
- 21 G. R. Desiraju, *Acc. Chem. Res.*, 2002, **35**, 565–573.
- 22 P. K. Thallapally and A. Nangia, *CrystEngComm*, 2001, **27**, 1–6.
- 23 D. Swierczynski, R. Luboradzki, G. Dolgonos, J. Lipkowski and H. J. Schneider, *Eur. J. Org. Chem.*, 2005, 1172–1177.

24 L. Brammer, E. A. Bruton and P. Sherwood, *Cryst. Growth Des.*, 2001, **1**, 277–290.  
25 E. J. Corey and T. W. Lee, *Chem. Commun.*, 2001, 1321–1329.  
26 G. Anitha and E. Subramanian, *Sens. Actuators, B*, 2005, **107**, 605–615.

27 Y. Chi, T. J. Peelen and S. H. Gellman, *Org. Lett.*, 2005, **7**, 3469–3472.  
28 F. Weinhold and C. R. Landis, *Chem. Educ.*, 2001, **2**, 91–104.  
29 S. R. Gadre, *Comput. Chem.*, 1999, **4**, 1–53.  
30 P.-W. Zheng, W. Wang and X.-M. Duan, *Acta Crystallogr., Sect. E*, 2005, **61**, 3020–3021.

# Chemical Biology

An exciting news supplement providing a snapshot of the latest developments in chemical biology



Free online and in print issues of selected RSC journals!\*

**Research Highlights** – newsworthy articles and significant scientific advances

**Essential Elements** – latest developments from RSC publications

**Free links** to the full research paper from every online article during month of publication

\*A separately issued print subscription is also available

30110553

RSC Publishing

[www.rsc.org/chemicalbiology](http://www.rsc.org/chemicalbiology)